2014 American Control Conference (ACC)
June 4-6, 2014. Portland, Oregon, USA

Application of Enthalpy-Based Feedback Control Methodology to the Two-Sided Stefan Problem*

Bryan Petrus, Joseph Bentsman, and Brian G. Thomas[1]

Abstract— **In [1], the authors introduced a novel control law for the single-phase Stefan problem, a nonlinear partial differential equation, with the eventual goal of applying the result to control of cooling in continuous steel casting. In this paper, the previously published method of controlling the Stefan problem is extended in two key ways that improve the fidelity of the nonlinear PDE as a model of the temperature and solidification of continuous steel casters. First, a non-symmetric temperature distribution is allowed, in which separate Neumann boundary control is applied at either surface. Two convergent control laws are compared in simulation, with one converging significantly faster. Second, saturation of the Neumann boundary control input is considered. Saturation is a significant concern in the actual process. The enthalpy-based algorithm still allows for convergence under saturation. However, as one would expect, severity of the constraints can affect the convergence rate.**

I. INTRODUCTION

According to industry statistics [2], 94.7% of steel produced in the world is made using the continuous casting process. This process is characterized by a continuous steel flow through the caster, called strand, that solidifies as it moves, allowing for high throughputs, but requiring stringent process control to maintain quality and safety.

The steel industry and researchers have long realized that temperature regulation is important to steel quality. The initial part of the caster - the mold - must contain the liquid steel long enough for a solid shell to grow around its boundaries. The mold must be vertical at the top to contain the liquid steel when it is poured into the caster. Therefore, the strand must be bent to horizontal so that it can be transported out of the caster for further processing. This causes transverse stresses on the surface of the steel that can lead to cracks. As the ductility of steel changes with temperature, preventing transverse surface cracks requires regulating the surface temperature of the steel [3].

At the same time, the liquid steel exerts hydrostatic pressure on the outer steel shell strong enough to bulge the shell outward. Inside the caster, bulging is prevented by containment rolls. If the steel has not fully solidified when it passes the last of these rolls, severe bulging occurs, known as a "whale" due to its shape, and liquid steel may even escape the shell. At best, production must be halted, while the whale is cut out by torches and removed by crane. In worse cases, the caster may be damaged or workers may even be injured by spouting liquid steel. To prevent this, the internal temperature of the steel must be below the melting temperature before the steel leaves containment.

Hence, proper control of this process requires that the temperature of the steel has a certain profile throughout the caster. That is, regulation of the distributed temperature profile of the steel strand is required. Standard heat conduction is modeled by a parabolic partial differential equation (PDE) that has been well-studied by control researchers [4], but with solidification this well-behaved PDE becomes nonlinear. One simple model of solidification is called the Stefan Problem, which breaks the spatial domain into time-varying subdomains representing liquid and solid material. The boundary between the domains moves over time according to an energy balance [5]. This model is naturally more difficult to analyze, and thus the literature on control of this process has roughly divided into two approaches: application-oriented approaches which use simplistic control algorithms that behave well but have no guarantee of performance, and control theoretical approaches that seek out guaranteed behavior but tend to rely on simplified control objectives or unrealistic actuation.

The current industry standard control method is actually open-loop control that changes the water spray rates in response to changes in casting speed, but not to grade, mold heat removal, initial temperature, or any other changing conditions. This open-loop control can be determined by experience, or through the use of offline optimization techniques such as [6], [7]. The most advanced controllers currently used in production consist of detailed computational models to predict the temperature of the steel, in order to overcome problems with sensor unreliability, and apply simple control laws. In [8], the authors invented a static nonlinear feedback rule based on repeated simulation trials. In [9], the authors applied multi-input multi-output PI control. Both focused on controlling the surface temperature to prevent transverse cracks, but neglect the whale problem. In [10], the authors applied PI control to the location of final solidification, which would prevent whales but not cracks. All three approaches focus primarily on the modelling difficulties, using a more detailed nonlinear PDE than the Stefan Problem, but apply off-the-shelf control laws and do not analyze their performance.

The other branch of research into this problem is in the control literature, rather than modelling. The approach used in [11] and [12] is to solve the inverse Stefan Problem, i.e. impose a desired trajectory of the boundary and determine computationally a temperature profile. This would clearly satisfy whale constraints, but could still result in temperature-related cracks. In [13], the authors determine necessary con-

*This work was supported by the Continuous Casting Consortium and NSF grant CMMI 1300907

[1]All authors are with the University of Illinois at Urbana-Champaign, Department of Mechanical Science and Engineering. Prof. Bentsman is the corresponding author, jbentsma@illinois.edu

ditions for receding horizon control for a nonlinear parabolic PDE that can describe solidification, but no results on either existence or stability of the optimal control are given. More concrete results on the subject have focused on the nonlinear Stefan Problem. In [14] and [15], the authors control the position of the solidification front, neglecting surface cracks, using thermostat-style boundary control inpus. In [1], the authors found a control law that ensured convergence of both temperature and solidification front position to a desired reference profile for a simplified Stefan problem that neglected some of the key challenges of the actual continuous casting process. In this paper, we extend the work of [1] by addressing some of these challenges.

In Section II we introduce the problem. We also restate the main convergence result from [1] and briefly sketch the proof. In Section III we extend the method to the two-sided Stefan problem. Finally, in Section IV, we investigate convergence when the Neumann boundary input is subject to saturation.

II. BACKGROUND

For a continuous caster, as described in [16], scaling analysis demonstrates that heat transfer by conduction in the casting (axial) direction is negligible compared to heat transfer by advection as material moves through the caster. Therefore, the temperature can be modeled by a transverse two-dimensional (2D) slice moving at the casting speed. In slab casters, the thickness is typically an order of magnitude smaller than the width, and so a one-dimensional (1D) slice will be accurate for most of the slab.

A. Control-oriented process model

In the Stefan Problem [5], which is a good model of solidification in ultra-low carbon steels, the slice is broken into two subdomains consisting of the liquid and solid phases of the strand. The position of the boundary between the two phases is denoted as $s(t)$. Then the following PDE models the evolution of temperature within the slice:

$$T_t(x,t) = aT_{xx}(x,t)\,, \quad x \in (0,\ell) - \{s\,(t)\}\,, \tag{1}$$

$$T(s\,(t)\,,t) = T_f, \quad T_x(0,t) = u(t)\,, \quad T_x(\ell,t) = 0, \tag{2}$$

$$T(x,0) = T_0(x) \tag{3}$$

$$\dot{s}(t) = b\left(T_x\big(s^-(t)\,,t\big) - T_x\big(s^+(t)\,,t\big)\right), \quad s(0) = s_0 \tag{4}$$

In physical terms, T_f is the melting temperature, a is the thermal diffusivity, and $b = k/\rho L_f$, where k is the thermal conductivity, ρ is the density, and L_f is the latent heat of fusion. All of these physical quantities are strictly positive. The control input u is applied as the left-hand side Neumann boundary condition. In the continuous caster, this is directly proportional to the heat flux removed from the steel at the surface.

The control objective for this process is to match a reference temperature $\bar{T}(x,t)$ and solidification front position $\bar{s}(t)$, that are the solutions to (1)-(4) under known reference control input $\bar{u}(t)$ with initial conditions $\bar{T}(x,0) = \bar{T}_0$ and $\bar{s}(0) = \bar{s_0}$. This reference profile can be designed, using for example offline optimization methods such as [6], [7], to give good quality steel under nominal conditions. Due to difference in pour temperatures and mold heat removal, however, the initial condition is actually not necessarily the same as the reference, and we seek a controller that converges the actual system state to the reference profile. We will denote the reference errors as $\tilde{T}(x,t) = T(x,t) - \bar{T}(x,t)$, and $\tilde{s}(t) = s(t) - \bar{s}(t)$. Also, we will denote $\tilde{u}(t) = u(t) - \bar{u}(t)$.

Symbol	Description	Value
a	thermal diffusivity	2.27×10^{-5} W/m · K
b	Stefan condition constant	4.13×10^{-8} m^2/K · s
T_f	melting temperature	1811 K
ℓ	half-thickness of strand	0.2 m
$\bar{u}$	constant reference input	3000 K/m

TABLE I
THERMODYNAMIC PROPERTIES USED IN SIMULATIONS

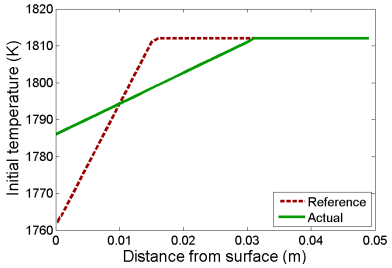

Fig. 1. Initial condition for simulations in Sections II and IV

In the presence of initial condition mismatch, if no control adjustment is made, the reference temperature error will reach a constant, non-zero steady state. This is illustrated in Figures 1 and 2. Note that there is an initial positive temperature error that quickly becomes negative due to the opposing error in solidification front position. This is a sign that enthalpy, meaning latent heat from the solidification front position error and sensible heat from the temperature, must both be considered. The physical parameters used in these simulations are given in Table I.

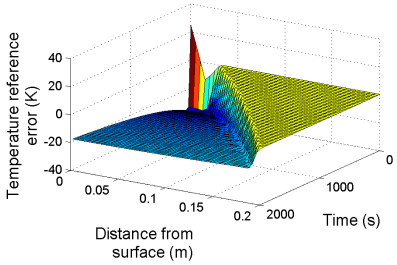

Fig. 2. Temperature error $\tilde{T}(x,t)$ with initial condition mismatch and no control adjustment

B. Enthalpy-based control algorithm

We make the following assumptions on both the reference and actual system:

1) [(A1)]
2) The initial conditions satisfy: $0 < s_0 < \ell$; T_0 is piecewise smooth, continuous, and nondecreasing; $T_0(x) < T_f$ for all $0 < x < s_0$ and $T_0(x) = T_f$ for all $x \geq s_0$.
3) The Neumann boundary input is bounded above and strictly positive: $\sup u(t) < \infty$. and $0 < \inf u(t)$

Assumption (A2) requires that the temperature in the liquid phase be constant. While not strictly true, in actual casting conditions the temperature in the liquid is negligible. A typical superheat (the difference between the initial temperature in the liquid and the melting temperature) is only around 25°C. In comparison, the average surface temperature of the steel in the caster is around 500°C less than the melting temperature. Moreover, due to fluid flow in the liquid, the temperature in the liquid reaches steady state much more quickly than conduction alone would achieve. A consequence of (A2) is that, in light of (4), $\dot{s}$ is non-negative.

Assumption (A3) is generally physically true. Since the strand is at a high temperature relative to the environment, there is always some heat lost due to radiation or convection even with no applied water sprays. The control algorithm found in [1] satisfies this assumption if the controller gain is small enough, and the effect of saturation is discussed in Section IV.

The main result of [1] is:

Theorem 2.1: Define the function:

$$h(T) \coloneqq \left\{ \begin{array}{ll} \frac{1}{a}T, & \text{if } T < T_f \\ \frac{1}{a}T + \frac{1}{b}, & \text{if } T \geq T_f \end{array} \right\}, \tag{5}$$

and denote

$$\tilde{H} \coloneqq \int_0^\ell \tilde{h}\,\mathrm{d}x = \frac{1}{a}\int_0^\ell \tilde{T}\,\mathrm{d}x - \frac{1}{b}\tilde{s}. \tag{6}$$

Let the reference and actual system both satisfy assumptions (A2) and (A3), and the Neumann boundary condition satisfies

$$u(t) = \bar{u}(t) + k\tilde{H}(t), \tag{7}$$

where gain $k > 0$. Then the reference temperature error $\tilde{T}$ converges asymptotically to 0 uniformly over the domain, and the interface position error $\tilde{s}$ converges to 0 asymptotically as well.

Proof: The following is a sketch of the proof. A detailed proof is given in [1].

First, note that taking the time derivative of $\tilde{H}$ using (1), (2), and (4), gives

$$\begin{aligned} \frac{\mathrm{d}}{\mathrm{d}t}\tilde{H} &= \int_0^\ell \tilde{T}_{xx} - \frac{1}{b}\dot{s} + \frac{1}{b}\dot{\bar{s}} \\ &= \tilde{T}_x\Big|_0^{s_1^-} + \tilde{T}_x\Big|_{s_1^+}^{s_2^-} + \tilde{T}_x\Big|_{s_2^+}^{\ell} + \tilde{T}_x\Big|_{s^-}^{s^+} + \tilde{T}_x\Big|_{\bar{s}^-}^{\bar{s}^+} \\ &= -\tilde{T}_x(0) + \tilde{T}_x(\ell) = -\tilde{u}. \end{aligned} \tag{8}$$

This calculation took advantage of the fact that the PDE (1) is linear and parabolic away from the moving boundary. Therefore, its solutions are piecewise continuous. As a consequence of (8), under control law (7), the quantities $\tilde{u}$ and $\tilde{h}$ are exponentially decaying. This means that k can be chosen sufficiently small enough so that assumption (A3) is satisfied.

In light of the bounded Neumann input and maximum principles for parabolic PDEs (see, e.g. [17]), $\tilde{T}_x$ is bounded uniformly, which then implies several further bounds. Using Poincare's inequality inequality given in [4] (Lemma 2.1, p. 17), we can find an upper bound on $\|T\|_2$. Since both T and T_x are bounded in the $L_2(0,\ell)$ norm, T is bounded in the Sobolev norm $H^1(0,\ell)$. Subsequently, Agmon's Inequality (Lemma 2.4, p. 20, *ibid*) ensures that $|T|$ is also uniformly bounded.

The main part of the proof uses an infinite-dimensional invariance principle from [18]. Consider the Lyapunov functional candidate

$$V\left(\tilde{T}\right) \coloneqq \frac{1}{2}\int_0^\ell \tilde{T}^2\,\mathrm{d}x - \frac{a}{b}T_f(s+\bar{s}) + 2\frac{a}{b}T_f\ell \tag{9}$$

on the state space of the error system, $\left(\tilde{T}, \tilde{s}\right) \in H^1(0,\ell) \times \mathbb{R}$. This function is clearly continuous on that space, and non-negative on trajectories of the system. The time derivative can be taken using (1)-(4) and integrating by parts. There are two moving boundaries in the error, from the reference and the actual systems. However, as mentioned above, the error will be linear and smooth away from those boundaries. Thus, we can eventually show

$$\begin{aligned} \frac{\mathrm{d}}{\mathrm{d}t}V\left(\tilde{T}\right) &= -a\tilde{T}(0)\,\tilde{u} - a\int_0^\ell \tilde{T}_x^2\,\mathrm{d}x \\ &\quad - \frac{a}{b}\left(\bar{T}(s)\,\dot{s} + T(\bar{s})\,\dot{\tilde{s}}\right) \\ &\leq -a\int_0^\ell \tilde{T}_x^2\,\mathrm{d}x. \end{aligned} \tag{10}$$

where the inequality follows from the facts, discussed above, that $\tilde{u}$ converges to 0 exponentially, $\tilde{T}$ is uniformly bounded, and $\dot{s}$ and $\dot{\tilde{s}}$ are both non-negative. More detail can be found in [1].

Once again applying Poincare's inequality:

$$\begin{aligned} -a\int_0^\ell \tilde{T}_x^2 dx &\leq -\frac{a}{4\ell^2}\int_0^\ell \tilde{T}^2\,\mathrm{d}x + 2\tilde{T}^2(\ell) \\ &= -\frac{a}{4\ell^2}\int_0^\ell \tilde{T}^2\,\mathrm{d}x, \end{aligned} \tag{11}$$

since $\tilde{T}(\ell) = T(\ell) - \bar{T}(\ell) = T_f - T_f = 0$. Using the fact that the state space of T, the Sobolev space H^1, can be compactly embedded in C^0 ([19], Theorem 5.5), and the invariance principle, $\tilde{T}$ converges to 0 uniformly. Since $\tilde{H}$ also converges to 0 and is defined as (6), so too must $\tilde{s}$. ■

III. EXTENSION TO TWO-SIDED STEFAN PROBLEM

As mentioned in Section I, the strand is bent from vertical to horizontal while in the caster. This means that spray water

will tend to pool on the top of the strand, but not the bottom, leading to significantly different heat transfer, and therefore a symmetric temperature distribution is not possible. Moreover, the inner and outer sides of the strand will undergo tensile stresses at different points within the caster (times, in the 1D moving slice model), so symmetric tensile distributions are not even necessarily desirable. Hence, we would like to drop the assumption of symmetry. The model (1)-(4) can be extended easily by including both sides of the caster, giving two moving solid-liquid boundaries and two Neumann boundary conditions.

$$T_t(x,t) = aT_{xx}(x,t)\,, \quad x \in (0,\ell) - \{s_1(t)\,, s_2(t)\}\,, \tag{12}$$

$$\begin{aligned} T(s_1(t)\,,t) = T_f = T(s_2(t)\,,t)\,, \\ T_x(0,t) = u_1(t)\,, \quad T_x(2\ell,t) = u_2(t)\,, \end{aligned} \tag{13}$$

$$T(x,0) = T_0(x) \tag{14}$$

$$\begin{aligned} \dot{s_1}(t) &= b\left(T_x\left(s_1^-,t\right) - T_x\left(s_1^+,t\right)\right), \quad s_1(0) = s_{1,0} \\ \dot{s_2}(t) &= b\left(T_x\left(s_2^-,t\right) - T_x\left(s_2^+,t\right)\right), \quad s_2(0) = s_{2,0}. \end{aligned} \tag{15}$$

Here, the material is liquid between s_1 and s_2, and solid otherwise. Assumption (A2) can be adjusted to reflect this.

1) [(A1)]
3) The initial conditions satisfy: $0 < s_{1,0} < s_{2,0} < 2\ell$; T_0 is piecewise smooth, continuous, and non-decreasing; $T_0(x) < T_f$ for all $x \in (0, s_{1,0}) \cup (s_{2,0}, 2\ell)$ and $T_0(x) = T_f$ for all $x \in (s_{1,0}, s_{2,0})$.

The reference profiles and errors can be defined equivalently.

A. Convergence Proof

For the two-sided Stefan problem, we can extend Theorem 2.1 to the following:

Theorem 3.1: Denote

$$\tilde{H_2} \coloneqq \int_0^{2\ell} \tilde{h}\,\mathrm{d}x = \frac{1}{a}\int_0^{\ell} \tilde{T}\,\mathrm{d}x + \frac{1}{b}\left(\tilde{s_1} - \tilde{s_2}\right). \tag{16}$$

Let the reference and actual system both satisfy assumptions (A3) and (A3), and the Neumann boundary conditions satisfy

$$\tilde{u_1}(t) + \tilde{u_2}(t) = k\tilde{H}(t)\,, \tag{17}$$

where gain $k > 0$. Then the reference temperature error $\tilde{T}$ converges asymptotically to 0 uniformly over the domain, and both interface position errors converge to 0 asymptotically as well.

Proof: The proof follows the same basic principle as the proof of Theorem 2.1. As in that case, the Neumann boundary control can be shown to directly affect the total enthalpy error.

$$\frac{\mathrm{d}}{\mathrm{d}t}\tilde{H} = -\tilde{u_1} - \tilde{u_2}. \tag{18}$$

So, the control law (17) drives the enthalpy error to 0.

We can show temperature convergence using the Lyapunov functional

$$\begin{aligned} V\left(\tilde{T}\right) \coloneqq \frac{1}{2}\int_0^{\ell} \tilde{T}^2\,\mathrm{d}x \\ - \frac{a}{b}T_f\left(s_1 + \bar{s_1}\right) - \frac{a}{b}T_f\left(s_2 + \bar{s_2}\right) \\ + 8\frac{a}{b}T_f\ell \end{aligned} \tag{19}$$

Taking the time derivative, using the PDE (12)-(15), and dividing by parts, we get

$$\begin{aligned} \frac{\mathrm{d}}{\mathrm{d}t}V\left(\tilde{T}\right) = -a\tilde{T}(0)\,\tilde{u_1} + a\tilde{T}(2\ell)\,\tilde{u_2} \\ - a\int_0^{2\ell} \tilde{T}_x^2\,\mathrm{d}x \\ - \frac{a}{b}\left(\bar{T}(s_1)\,\dot{s_1} + T(\bar{s_1})\,\dot{\bar{s}_1}\right) \\ - \frac{a}{b}\left(\bar{T}(s_2)\,\dot{s_2} + T(\bar{s_2})\,\dot{\bar{s}_2}\right) \end{aligned} \tag{20}$$

To complete the proof, we need the bounds on $\tilde{T}$ and $\tilde{T}_x$ that came from Poincare's and Agmon's inequalities. These relied on knowing that $\tilde{T}(\ell) = 0$ due to symmetry, which is not necessarily true any more.

There are two possible cases. First, the liquid phases of the reference and actual system overlap at some point, i.e. $T(x_{eq}) = \bar{T}(x_{eq}) = T_f$, for some $0 < x_{eq} < 2\ell$. Second, there is no overlap. This necessarily means that $s_2 < \bar{s_1}$, or $s_1 > \bar{s_2}$. If the former is true, Assumption (A3) means that $T(s_2) = T_f$ and $T(\bar{s_1}) < T_f$, while $\bar{T}(s_2) < T_f$ and $\bar{T}(\bar{s_1}) = T_f$, and the two temperature profiles are continuous. Therefore, they must intersect at some point $s_2 < x_{eq} < \bar{s_1}$. Similar reasoning holds if $s_1 > \bar{s_2}$. Thus, we must have a point where the temperatures are equal, and $\tilde{T}(x_{eq}) = 0$, which allows us to apply Poincare's and Agmon's inequalities.

The remainder of the proof follows the same as for Theorem 2.1. ∎

Unfortunately, as illustrated below, convergence under this proof is not necessarily guaranteed until after final solidification occurs.

B. Simulation Results and Discussion

In this section we will compare two algorithms for control of the two-sided Stefan problem:

$$\tilde{u_1} = \tilde{u_2} = \frac{k}{2}\left(\frac{1}{a}\int_0^{\ell} \tilde{T}\,\mathrm{d}x + \frac{1}{b}\left(\tilde{s_1} - \tilde{s_2}\right)\right), \tag{21}$$

and

$$\begin{aligned} \tilde{u_1} &= k\left(\frac{1}{a}\int_0^{\ell} \tilde{T}\,\mathrm{d}x + \frac{1}{b}\tilde{s_1}\right) \\ \tilde{u_2} &= k\left(\frac{1}{a}\int_{\ell}^{2\ell} \tilde{T}\,\mathrm{d}x - \frac{1}{b}\tilde{s_2}\right). \end{aligned} \tag{22}$$

Note that both (21) and (22) meet the criteria (17) for Theorem 3.1. However, suppose the initial condition has an error as shown in Figure 3. Since the error in enthalpy is

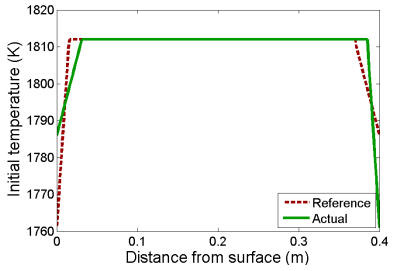

Fig. 3. Initial condition for simulations in Section III-B

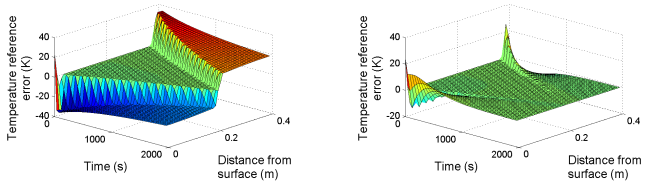

(a) Using Neumann boundary control (21)

(b) Using Neumann boundary control (22)

Fig. 4. Temperature error $\tilde{T}$ for two-sided Stefan Problem (12)-(15), with initial conditions from Figure 3 and different boundary control

symmetric, the control law (21) will not make any adjustment. The errors will eventually converge, but not until after final solidification, as shown in Figure 4a. For the intended application of continuous casting, convergence this slow will fail to meet the quality and safety goals.

Compare this with control law (22), which is simulated in Figure 4b. The second control law converges before final solidification. While these initial conditions are unrealistic, they illustrate the importance of considering the convergence rate when using this control method.

IV. CONVERGENCE UNDER INPUT SATURATION

An additional concern in actual casting applications is actuator saturation. The steel is cooled by water sprays, and there are a strict upper and lower bounds on the spray rates. The upper bound comes from the limits of the piping system, and the lower bound from the minimum water flow rate necessary to produce a steady spray fan. In [1], it is suggested that this may be dealt with by decreasing the controller gain k. However, due to clogging, loss of pressure, or other problems, the saturation bounds may even not be known. We would like to know whether the control law works if saturation is applied. So, we will use the notation

$$u_{sat} \coloneqq \begin{cases} u_L, & \text{if } u \leq u_L \\ u, & \text{if } u_L \leq u \leq u_U \\ u_U & u \geq u_U \end{cases} \tag{23}$$

For simplicity, we will prove the following results on the single-sided Stefan problem, but it is straight-forward to extend them to the two-sided problem.

A. Convergence Proof

It turns out that the enthalpy-based control algorithm will still converge, as long as some control adjustment is possible around the reference profile. Specifically:

Theorem 4.1: Let u and u_{sat} be defined as in (7) and (23) respectively. Suppose there exists $\varepsilon > 0$ such that

$$u_L < \bar{u} \pm \varepsilon < u_U \tag{24}$$

for all time, and T and s satisfy system (1)-(4) with boundary condition $T_x(0,t) = u_{sat}$, then T converges uniformly to $\bar{T}$ and s converges to $\bar{s}$.

Proof: In order to simplify notation, we will continue to let $\tilde{u}$ denote the error between the desired control effort and the reference control, and denote $\tilde{u}_{sat} \coloneqq u_{sat} - \bar{u}$ for the difference under actuator saturation. Using this notation, the derivative of $\tilde{H}$, calculated in (8), becomes

$$\frac{\mathrm{d}}{\mathrm{d}t}\tilde{H} = -\tilde{u}_{sat} \tag{25}$$

If

$$-\varepsilon < \tilde{u}(t) = k\tilde{H}(t) < \varepsilon, \tag{26}$$

at any time t, then (24) ensures $u_L \leq u \leq u_U$ and saturation does not occur, i.e. $\tilde{u} = \tilde{u}_{sat}$. In this case, (25) is the same as the calculation (8) in the proof to Theorem 2.1, so the conditions for the proof still hold. Under those conditions, (7), $\tilde{u}$ is exponentially decreasing, and so (26) will continue to hold, the boundary control input will never saturate, and convergence occurs as normal.

If saturation does occur, then either $\tilde{u}_{sat} = u_L - \bar{u}$ or $\tilde{u}_{sat} = u_U - \bar{u}$. In either case, (24) ensures that $\tilde{u}_{sat} \geq \varepsilon$ and furthermore

$$\operatorname{sign}(\tilde{u}_{sat}) = \operatorname{sign}(\tilde{u}) = \operatorname{sign}\left(k\tilde{H}\right) = \operatorname{sign}\left(\tilde{H}\right)$$

and also that $|\tilde{u}_{sat}| \geq \varepsilon$ Therefore, using (25),

$$\frac{\mathrm{d}}{\mathrm{d}t}\left|\tilde{H}\right| = \frac{\frac{\mathrm{d}}{\mathrm{d}t}\tilde{H}}{\operatorname{sign}\left(\tilde{H}\right)} = \frac{-\tilde{u}_{sat}}{\operatorname{sign}(\tilde{u}_{sat})} = -\left|\tilde{u}_{sat}\right| \leq -\varepsilon.$$

Therefore, the magnitude of $\tilde{H}$ is strictly decreasing, and eventually (26) will be true. ■

B. Simulation Results and Discussion

The condition (24) simply requires that there be some actual control adjustment available. As long as there is any consistent room, however small, between the reference control and the saturation bounds, the error will converge to 0. Under this assumption, the enthalpy error will still move towards 0 until it is close enough that control law (7) does not saturate. Figures 5a–5c illustrate this convergence. The parameters used are given in Table I, and the initial conditions are in Figure 1. The saturation bounds are $u_L = 2500$ W/m $\cdot$ K and $u_U = 3500$ W/m $\cdot$ K. As proven, despite saturation, the reference errors still converge to 0.

An important extension of this result is to the case where the saturation bounds are time-varying.

$$u_{sat} \coloneqq \begin{cases} u_L(t), & \text{if } u \leq u_L(t) \\ u, & \text{if } u_L(t) \leq u \leq u_U(t) \\ u_U(t) & u \geq u_U(t) \end{cases} \tag{27}$$

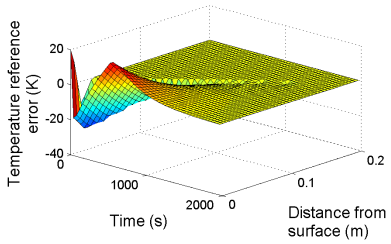

(a) Temperature error $\tilde{T}$ with actuator saturation

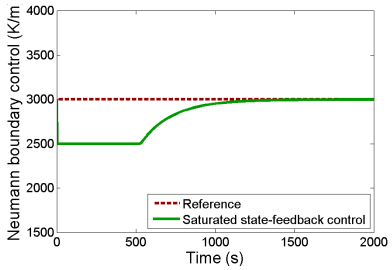

(b) Neumann boundary control with actuator saturation.

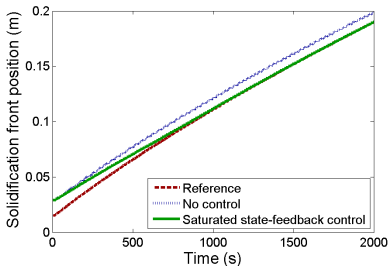

(c) Solidification front position $s(t)$, comparing result with no control and (7) under saturation.

Fig. 5. Illustration of Theorem 4.1 by numerical simulation of Stefan Problem (1)-(4), with initial conditions from Figure 1 and Neumann boundary control (7) under saturation.

This should be considered because of the containment rolls mentioned in Section I. While the slice is under the containment rolls, the sprays cannot reach the surface. The sprays have an indirect effect by drawing heat from the rolls, but the upper bound is very small. However, the key to convergence is still to match the enthalpy. That is,

Theorem 4.2: Let u and u_{sat} be defined as in (7) and (27) respectively. Suppose the saturation bounds $u_L(t)$ and $u_U(t)$ satisfy

$$\int_0^\infty (u_L - \bar{u})\, \mathrm{d}t \leq \tilde{H}(0) \leq \int_0^\infty (u_U - \bar{u})\, \mathrm{d}t \qquad (28)$$

and T and s satisfy system (1)-(4) with boundary condition $T_x(0,t) = u_{sat}$. Then, if k is sufficiently large, T converges uniformly to $\bar{T}$ and s converges to $\bar{s}$.

Proof: The proof follows the same ideas as Theorem 4.1, and is omitted due to space limitations. ■

The condition (28) is more difficult to verify than condition (24). Moreover, even if the condition is satisfied, a concern will be whether the rate of convergence is sufficiently fast to allow the quality and safety goals to be met. This is the subject of ongoing work. Another important weakness of these results is the reliance on full-state, rather than more realistic boundary temperature sensing. While numerically–supported output feedback laws were presented in [20] and [1], their convergence is yet to be proven and is still being investigated.

ACKNOWLEDGMENT

We gratefully acknowledge Professor Semyon Meerkov of the University of Michigan for a conversation that led to the development of Section IV.

REFERENCES

[1] B. Petrus, J. Bentsman, and B. Thomas, "Enthalpy-based feedback control of the stefan problem," in *51st Conference on Decision and Control*, (Maui, HI), December 2012.

[2] "Steel statistical yearbook 2012." `http://worldsteel.org`, 2012.

[3] M. M. Wolf, *Continuous Casting: Initial Solidification and Strand Surface Quality of Peritectic Steels*, vol. 9. Warrendale, PA: Iron and Steel Society, 1997.

[4] M. Krstic and A. Smyshlyaev, *Boundary Control of PDEs: A course on Backstepping Designs*. Philadelphia: SIAM, 2008.

[5] L. I. Rubinstein, *The Stefan Problem*. Providence, RI: American Mathematical Society, 1971.

[6] M. Hinze and S. Zigenbalg, "Optimal control of the free boundary in a two-phase Stefan problem," *Journal of Computational Physics*, vol. 223, pp. 657–684, 2007.

[7] C. Saguez, *Optimal control of free boundary problems*, pp. 776–788. Heidelberg: Springer Berlin, 1986.

[8] R. Hardin, K. Liu, A. Kapoor, and C. Beckermann, "A transient simulation and dynamic spray cooling control model for continuous steel casting," *Metal. and Material Trans.*, vol. 34B, pp. 297–306, 2003.

[9] B. Petrus, K. Zheng, X. Zhou, B. Thomas, and J. Bentsman, "Metallurgical and materials transactions b," *Real-Time Model-Based Spray-Cooling Control System for Steel Continuous Casting*, vol. 42B, no. 2, pp. 87–103, 2011.

[10] B. Furenes and B. Lie, "Solidification and control of a liquid metal column," *Simulation Modelling Practice and Theory*, vol. 14, pp. 1112–1120, 2006.

[11] W. B. Dunbar, N. Petit, P. Rouchon, and P. Martin, "Motion planning for a nonlinear Stefan problem," *ESAIM: Control, Optimisation and Calculus of Variation*, vol. 9, pp. 275–296, 2003.

[12] N. Petit, *Advances in the Theory of Controls, Signals and Systems with Physical Modeling*, ch. Control Problems for One-Dimensional Fluids and Reactive Fluids with Moving Interfaces, pp. 323–337. Berlin: Springer, 2010.

[13] T. Hashimoto, Y. Yoshioka, and T. Ohtsuka, "Receding horizon control with numerical solution for nonlinear parabolic partial differential equations," *IEEE Transactions on Automatic Control*, vol. 58, no. 3, pp. 725–730, 2013.

[14] K.-H. Hoffmann and J. Sprekels, *Real-time control of a free boundary problem connected with the continuous casting of steel*, pp. 127–143. Basel, Switzerland: Birkhauser, 1984.

[15] P. Colli, M. Grasselli, and J. Sprekels, "Automatic control via thermostats of a hyperbolic stefan problem with memory," *Applied Mathematics and Optimization*, vol. 39, pp. 229–255, 1999.

[16] Y. Meng and B. G. Thomas, "Heat transfer and solidification model of continuous slab casting: Con1d," *Metallurgical and Material Transactions B*, vol. 34, pp. 685–705, 2003.

[17] O. A. Ladyzenskaja, V. A. Solonnikov, and N. N. Uralceva, *Linear and Quasilinear Equations of Parabolic Type*. Providence, Rhode Island: American Mathematical Society, 1968.

[18] J. A. Walker, *Dynamical Systems and Evolution Equations: Theory and Applications*. New York: Plenum Press, 1980.

[19] L. C. Evans, *Partial Differential Equations*. Providence, Rhode Island: American Mathematical Society, 1998.

[20] B. Petrus, J. Bentsman, and B. Thomas, "Feedback control of the stefan problem with an application to continuous casting of steel," in *49th Conference on Decision and Control*, (Atlanta, GA), December 2010.